

# SmartHat: A Battery-free Worker Safety Device Employing Passive UHF RFID Technology

Stewart Thomas  
Department of Electrical and  
Computer Engineering  
Duke University  
Durham, North Carolina

Jochen Teizer  
School of Civil and  
Environmental Engineering  
Georgia Inst. of Tech.  
Atlanta, Georgia

Matthew Reynolds  
Department of Electrical and  
Computer Engineering  
Duke University  
Durham, North Carolina

**Abstract**—In many safety-critical applications, battery performance is a significant limiting factor that affects the feasibility of electronic safety devices intended to alert workers to hazardous situations. In particular, battery capacity and lifetime are difficult to predict when safety devices are exposed to extremes of temperature, humidity, shock, and vibration that are common in construction, excavation, drill rigs, and mining work sites. Because battery failure is unacceptable in safety devices, periodic preventative maintenance is required, adding to device cost and labor cost and reducing acceptance of electronic safety devices.

Energy harvesting and communications techniques based on passive UHF RFID technology may offer an alternative to battery power for some types of safety alert devices, particularly where hazardous conditions are created by powered heavy equipment. We present a worker safety device designed around a passive UHF RFID platform that derives its operating power from specialized interrogators mounted on heavy equipment. This device is designed to be integrated with plastic hard hats that are commonly used in the construction industry to yield an intelligent hard hat, called a “SmartHat”, that delivers an audible alert directly to workers in proximity to a particular piece of equipment. It is addressable using an ASK interrogator-to-tag link, and backscatters confirmation that an alert has been delivered to the worker.

We present the design of the SmartHat tag, including a compact printed-circuit vee style antenna, an RF-to-DC power harvesting circuit, and a microprocessor-driven alert speaker. The tag’s average operating power while delivering a pulsed alert is 1.8 V at 61  $\mu$ A, or 110  $\mu$ W (−9.6 dBm). Its power-up threshold when not delivering an alert is 1.8 V at  $\approx$  10  $\mu$ A. We also present a specialized interrogator device operating under FCC Part 18 rules in the 902–928 MHz band that is mounted to a piece of construction equipment to power and communicate with nearby SmartHats. In outdoor testing of the SmartHat tag and its companion interrogator device, +35 dBm transmitter output power feeding a 9 dBi Yagi antenna (+44 dBm EIRP) allows for safety alerts to be delivered at distances of up to 16.46 m.

## I. INTRODUCTION

When working near powered heavy equipment commonly found on construction, excavation, drill rigs, and mining work sites, workers must always be aware of their environment and surroundings. This situational awareness is difficult for workers and machine operators to maintain on busy, noisy work sites, particularly under challenging environmental conditions such as night work in fog, rain, or snow, or work in a mine or on an offshore drill rig. Unintended contact between workers and heavy equipment can result in death or severe injury to

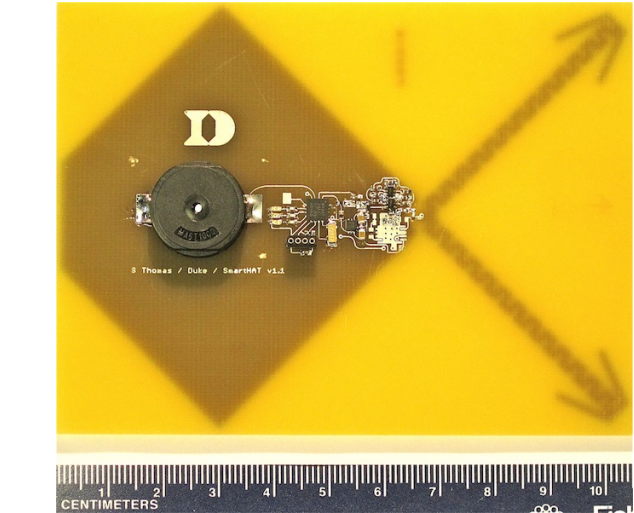


Fig. 1. The SmartHat battery-free worker safety device

workers. Some of these accidents could be avoided if a worker could be given a targeted warning or alert to a nearby hazard.

Current electronic safety warning devices such as [1]–[3] are worn on a user’s belt and provide an audible alert when a transmitter-equipped hazard is in proximity to the worker. The early warning provided by these devices allows time for the worker move to safety and avoid an accident. However, most currently available electronic safety alert devices suffer from being positioned on the body at waist level, reducing the audibility of the device’s alarm, and require periodic battery inspection and replacement to ensure functionality. A major contribution to the bulky size and weight of the device is the battery that is required for operation. On a large job site there may be hundreds or thousands of batteries to periodically check and replace, which has a high recurring battery and labor cost. Environmental impact of used batteries is also a concern because alkaline batteries, which have the least environmental impact of common battery technologies, have very poor performance over temperature. A common EN-91 type AA alkaline battery [4] is only specified for storage or operation from −18°C to +55°C (0°F to +130°F). Lithium batteries [5] have a much broader operating temperature range

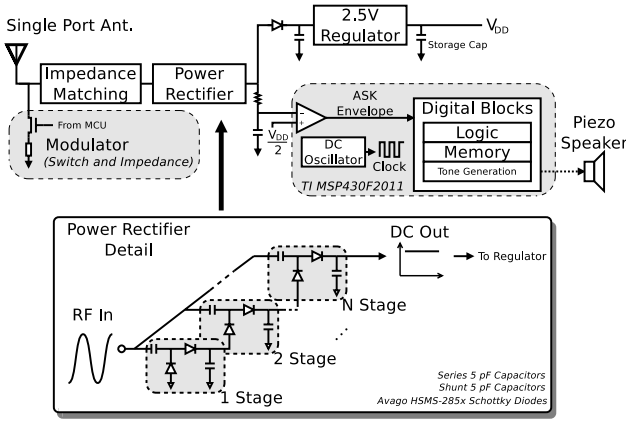


Fig. 2. Block diagram of the SmartHat tag

of  $-40^{\circ}\text{C}$  to  $+60^{\circ}\text{C}$  ( $-40^{\circ}\text{F}$  to  $+140^{\circ}\text{F}$ ) and are much more suitable for this application. In any case, used batteries must be collected for proper disposal, especially in the case of lithium batteries which may be dangerous if accumulated in large quantities.

In this paper we present the SmartHat tag (Fig. 1), a passive, maintenance-free safety device designed to avoid these problems by eliminating the battery from the safety device. The SmartHat tag consists of a printed circuit board containing surface mount components ( $7.6\text{ cm} \times 10.5\text{ cm} \times 2.5\text{ mm}$ ) and is designed for placement inside an OSHA-approved worker hard hat. The SmartHat tag circuitry includes a reduced-size printed-circuit vee style antenna, an RF-to-DC power harvesting circuit, a backscatter modulator, and a microprocessor-driven piezoelectric speaker. The SmartHat hardware is conceptually similar to a WiSP tag [6], [7], although the WiSP tag relies on an external dipole antenna and does not include an output device such as the piezoelectric speaker used in the SmartHat. Furthermore, due to its specialized application, the SmartHat tag need not be compatible with existing RFID communication protocols, and this allows lower power consumption than the WiSP's ISO18000-6c protocol implementation due to reduced clock rate requirements on the tag. We also present a specialized interrogator device operating under FCC Part 18 rules in the 902-928MHz band that is mounted to a piece of construction equipment to power and communicate with nearby SmartHats.

## II. SMARTHAT SYSTEM COMPONENTS

The system consists of two main components: an interrogator device that is mounted to and powered by a piece of heavy machinery, and the SmartHat tag which is installed in a worker hardhat. Like an ordinary passive UHF RFID tag, the operating power for the SmartHat is provided by the interrogator-to-tag downlink channel. The block diagram of the SmartHat tag is presented in Fig. 2. RF energy is collected by the planar antenna, converted to a DC operating voltage ranging from 1.8V at power-up threshold to 2.5V at regulation limit, and used to power a 16-bit Texas Instruments MSP430F2011 microcontroller. The MSP430 handles audible tone generation

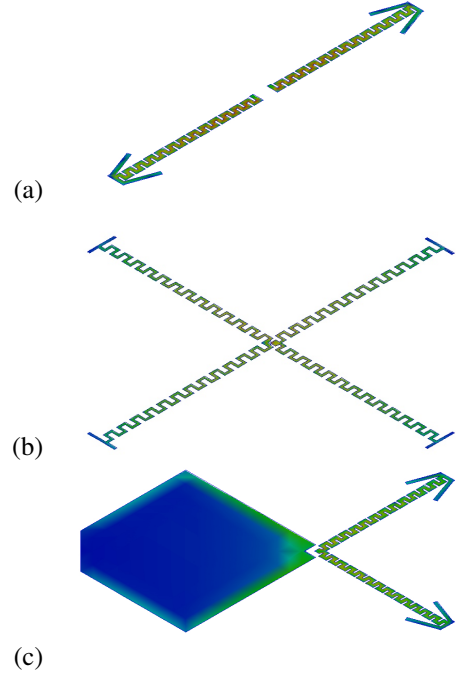


Fig. 3. Geometry and current distribution for the a) meandered dipole b) “X” and c) “Vee” style antennas

and communication with the interrogator device through an on-chip oscillator for clock signal generation and internal comparator for reader-to-tag ASK demodulation.

### A. Tag Antenna Design

The SmartHat includes a planar antenna designed to operate over the 902-928 MHz band. Because of the available space inside the crown of the hard hat, a reduced size antenna is required with the plane of the SmartHat PCB being horizontal. Because the direction of incident radiation will vary in azimuth according to the worker’s bearing with respect to the construction equipment, the antenna is designed for horizontal polarization with as omnidirectional performance as possible.

Antenna design was performed using the method-of-moments solver (Momentum) in Agilent ADS. Design iteration began with a meandered dipole configuration, shown in Fig. 3(a), which has broad, deep nulls over azimuth as shown in Fig. 4(a). To better trade off null depth at the expense of gain, and to yield a lower impedance that could be matched more easily to the power harvester, an “X” configuration was then simulated as shown in Fig. 3(b). This “X” configuration was fabricated but was found to be very sensitive to the surface mounted components on the opposite side of the PCB. The final configuration selected for the SmartHat antenna is a “Vee” configuration as shown in Figures 1(c) and 3(c), which has the advantage of a large copper region of low current density. Components could be easily placed toward the center of the large copper region which provides a good ground plane for the RF components while minimizing interaction between the other components and the antenna itself.

To determine the radiation patterns of the antenna, the test

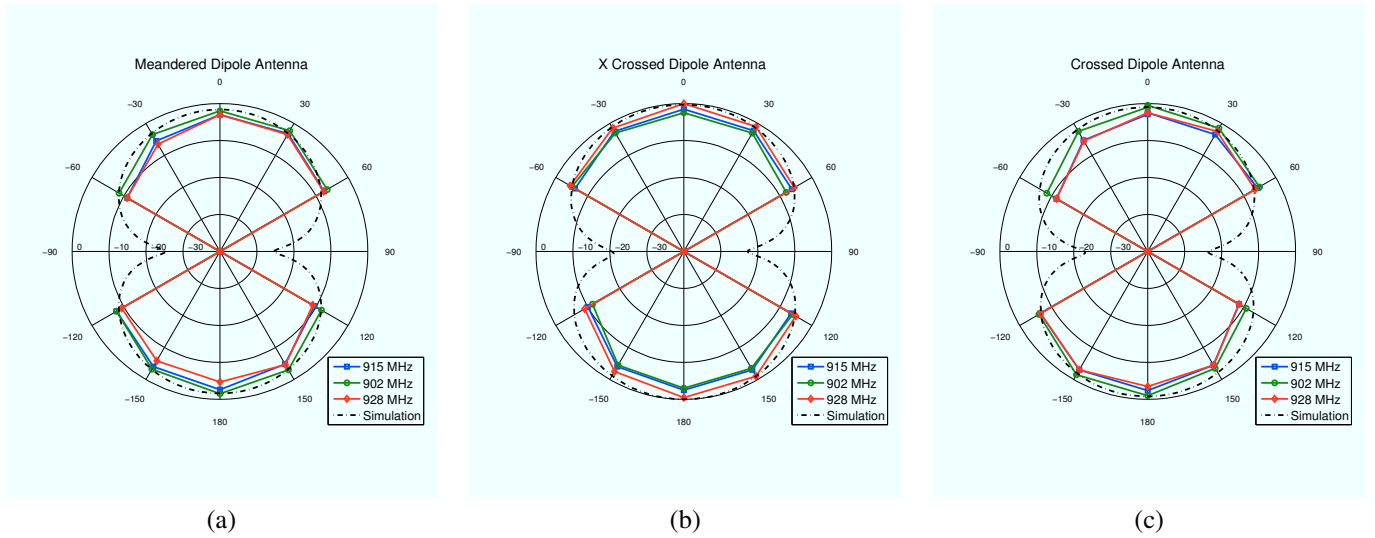


Fig. 4. Measured vs. simulated radiation patterns of three antenna geometries: a) single dipole b) “X” and c) “Vee”

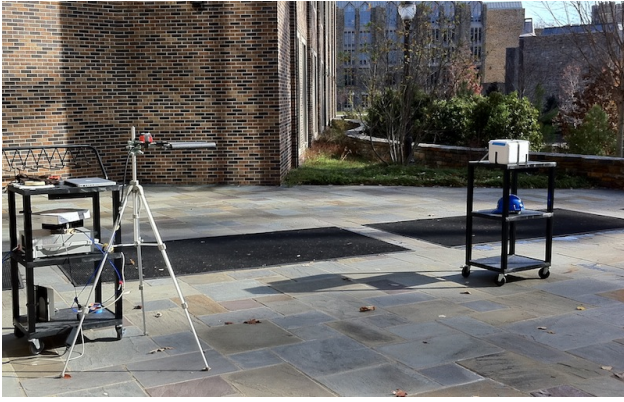


Fig. 5. Outdoor antenna test setup

setup of Fig. 5 was employed. Each tag was placed atop a styrofoam container on a plastic cart, at a fixed distance (3m) away from the transmitter. Transmitter power was increased until the alert from the SmartHat was heard, thus determining the power-up threshold of the tag as a function of azimuth angle. By recording this alert threshold power, the tag’s radiation patterns could be measured without a physical connection to the circuit under test. These measured radiation patterns were then scaled with a fixed offset correction and compared with the results from the method-of-moments simulation as shown in Fig. 4. The peak gain of this family of reduced size antenna was around 0 dBi including substrate and copper losses.

### B. RF to DC Conversion

Unlike an ordinary passive UHF RFID tag, the SmartHat tag includes a piezo speaker. When an alert sound is generated, a high peak current is consumed due to the duration of the audio tone driving the attached speaker lasting for several milliseconds. This results in a complex tradeoff between optimizing the power harvester for operation at the microcontroller’s power-up threshold (1.8 V at  $\approx 10 \mu\text{A}$ ), or the much higher

power required during alert tone generation (1.8 V at  $61 \mu\text{A}$ ). While adding stages to the voltage multiplier would permit the MSP430 to awaken from sleep at a much lower incident RF power, insufficient power would be available to deliver the audible alert at that operating point. The SmartHat’s harvester was therefore optimized around the operating point needed for alert generation at the  $40 \text{ k}\Omega$  load point, because the tag would be useless as a safety alert device unless sufficient incident power were available to drive the speaker for an extended period of time. This provides good performance during both sleep mode as well as active mode when generating the audible tone.

The power harvesting circuit is a multi-stage voltage multiplier connected to the antenna via a matching network. Simulations using Agilent ADS models for the Avago HSMS28x series Schottky diodes have good agreement with experimental data and were used to choose the total number of multiplier stages. As shown in Fig. 6, the open-circuit output voltage from the voltage multiplier varies widely over the expected incident power range of -10 dBm to over +10 dBm. To deliver the MSP430’s power-up threshold voltage of 1.8 V, an input power of approximately -9 dBm is required from either a 1-stage doubler or 4-stage voltage multiplier. At low input power, non-ideal impedance matching as well as the increased series forward voltage drop contributed by each additional diode tends to result in diminishing efficiency for each additional stage.

Since the charge pump is not an ideal voltage source, its power conversion efficiency and performance is affected by the load attached to the output [8]–[10], which in the case of the SmartHat tag is dominated by the power consumption of the MSP430 and the piezo speaker when an alert is being delivered. Using Agilent ADS to sweep the number of rectification stages, RF input power, and load value, the efficiency as well as the power-up threshold RF input was calculated for 2-6 voltage multiplier stages. The optimal number of stages as a



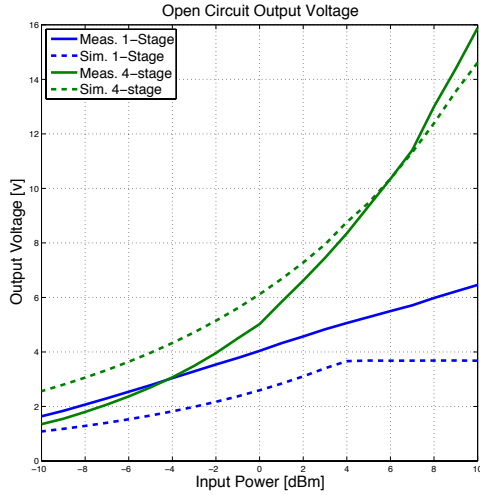


Fig. 6. Matched open-circuit voltage at multiplier output, HSMS285 diodes

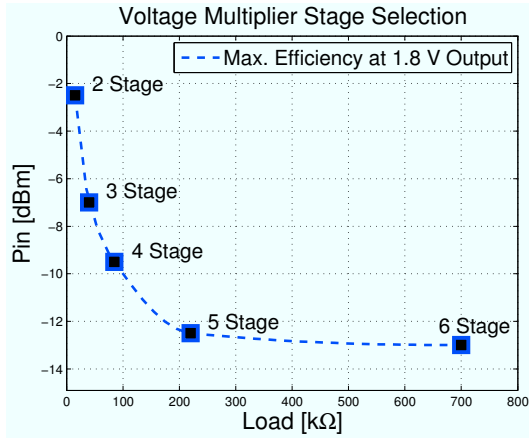


Fig. 7. Voltage multiplier efficiency vs. input power, number of stages, and load impedance

function of input power and load impedance while delivering a minimum of 1.8 V to the load is shown in Fig. 7. A 4-stage voltage multiplier was implemented in the SmartHat device because it delivered the highest RF-DC conversion efficiency near the 40 k $\Omega$  load impedance point, which is the approximate load impedance of the SmartHat digital circuitry and piezo speaker when delivering an alert sound. At higher input power (above approximately -4 dBm) a shunt regulator limits the voltage delivered to the microcontroller to 2.5 V. A small ceramic storage capacitor of 10  $\mu$ F is charged by the voltage multiplier and provides a charge reservoir for device operation. Larger capacitors, particularly electrolytics or wet-dielectric supercapacitors, are avoided because they typically have increasing leakage at high temperatures and a limited operational lifetime under severe thermal cycling as can occur in harsh environments.

### C. Modulation and Demodulation

Interrogator to SmartHat communication is accomplished by means of ASK (forward link) and PSK backscatter (return

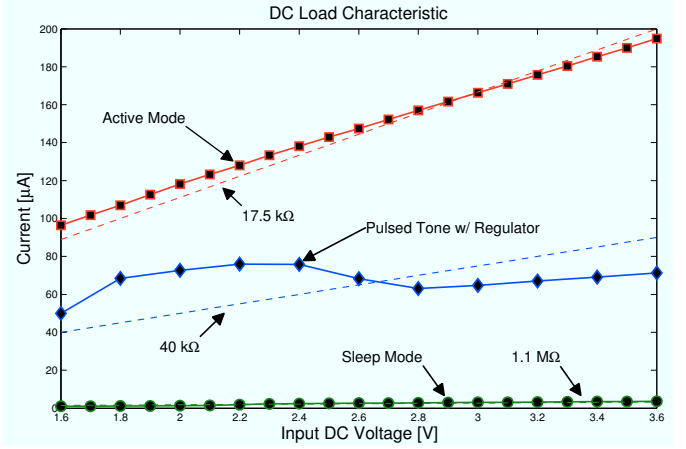


Fig. 8. I-V curve of the SmartHat tag circuitry in different operating modes

link) in exactly the same manner as a traditional passive UHF RFID tag. For demodulation, an internal node of the power harvester is isolated by means of an extra diode and connected to a comparator input pin of the SmartHat's MSP430 microcontroller. The comparator threshold is set such that 25-100% ASK of the forward link is detected by the MSP430. A modulating enhancement mode RF switching FET controlled by the MSP430 switches a small capacitance ( $\approx$  3 pF including parasitics) in parallel with the antenna terminals to introduce modulated backscatter for the return link.

### D. DC Power Characterization

The SmartHat's MSP430F2011 microcontroller alternates between a low-power sleep mode (LPM3) and a low duty cycle pulsed tone mode (LPM2) where a tone signal is generated and sent to a piezoelectric speaker. To determine the load characteristics of the microcontroller and piezo speaker in sleep, pulsed tone, and active modes, the MSP430 was forced into different operating modes and its I-V curve measured as shown in Fig. 8. These measurements reflect the total DC current consumed by the microcontroller, the 2.5 V regulator, and all other circuit components. The effective load varies between 17.5 k $\Omega$  when in 80 kHz active mode - which is only entered by the SmartHat firmware during pulsed tone generation, and roughly 1 M $\Omega$  in LPM3. When generating the audio alert, the average effective impedance of the circuit is  $\approx$  40 k $\Omega$  for DC input supply levels less than 3 V.

Because the SmartHat tag does not implement a high data rate communication protocol (e.g. the ISO18000-6c protocol), its clock rate can be far lower than would be required for those applications. Initial SmartHat prototypes operate at an active mode clock of 80 kHz which is higher than necessary to provide the alert function. The duty cycle of the MCU core is kept low, especially during audio alerts, to maximize power delivery to the piezo speaker.

At the alert threshold, on average 6  $\mu$ A are consumed by the demodulation branch (including 3.3  $\mu$ A for reference generation), 29  $\mu$ A consumed by the regulator, 20  $\mu$ A consumed by the microcontroller, and 6  $\mu$ A by the piezo speaker for a total

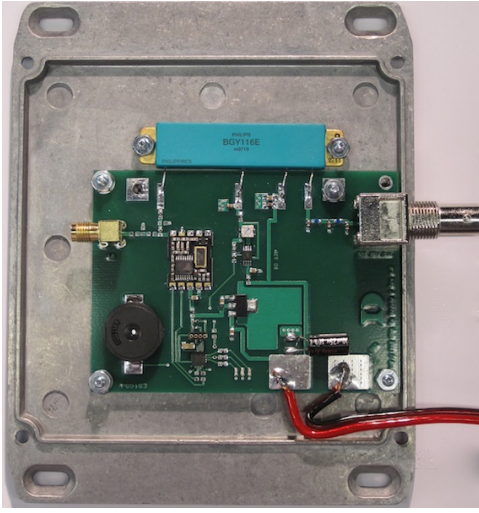


Fig. 9. Equipment-Mounted Interrogator Device

of  $61 \mu\text{A}$  at  $1.8\text{V}$  or  $110\mu\text{W}$ . As the harvested voltage increases towards the  $2.5\text{V}$  regulation level, the total consumed power rises to approximately  $170\mu\text{W}$  and remains constant until the input level is near  $3\text{V}$ . This power consumption curve is in large part due to the quiescent current of the  $2.5\text{V}$  series VDD regulator.

### III. EQUIPMENT-MOUNTED INTERROGATOR

A UHF interrogator device shown in Fig. 9 has been designed to provide power and communication to the SmartHat tags. Unlike many UHF RFID interrogators, the SmartHat interrogator device is very simple because it is not part of a networked installation. Each interrogator unit operates independently and communicates only with nearby SmartHat tags. This interrogator is optimized for low cost, simplicity, and independence from any external infrastructure other than its operating power. This enhances reliability when compared with traditional UHF RFID interrogators which have very complex operating system software (e.g. Windows Embedded or Linux) which can lead to instability that would be unacceptable in a safety alert device. Because of the high power consumption of the SmartHat tag when delivering an audio alert ( $110\mu\text{W}$ ) compared to typical UHF RFID tags ( $\approx 10\mu\text{W}$ ) a much higher EIRP is required to achieve similar operating distances. The SmartHat interrogator is able to deliver an RF output power of up to  $+36\text{dBm}$  and is typically used with antenna gain of  $8\text{-}10\text{dBi}$ , yielding an EIRP of up to  $+46\text{dBm}$ . These power levels exceed the FCC Part 15.247 EIRP limit of  $+36\text{dBm}$  EIRP, but are permitted under site license per FCC Part 18 rules.

A block diagram of the transmit portion of the interrogator device is shown in Fig. 10. The receive portion of the device has not yet been implemented, but will be needed to acknowledge that a worker alert has been delivered. This acknowledgment would be useful for evaluating the reliability of message delivery even though it may not have an impact on the practical usability of the device since there is no

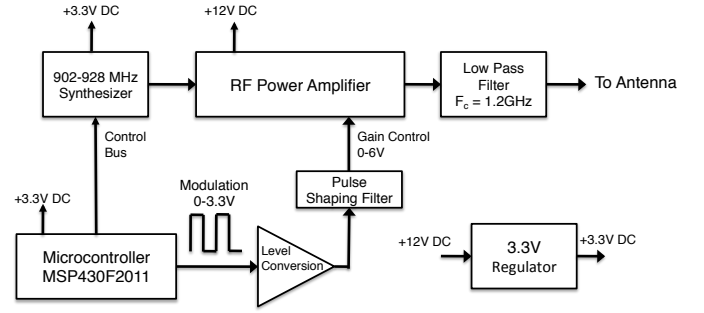


Fig. 10. Interrogator block diagram

way to distinguish an absent worker from a missed alert. An MSP430F2011 microcontroller is used to control the transmit module. The microcontroller programs the frequency synthesizer to generate a  $902\text{-}928\text{MHz}$  carrier, which is amplified by a rugged power amplifier module specified for continuous duty at  $+36\text{dBm}$  output. The interrogator's MSP430 can also amplitude modulate the power amplifier to send addressing commands from the interrogator to the SmartHat tags. This capability is useful when selectively addressing only certain groups of SmartHat tags. For example, a heavy equipment operator's SmartHat should not be triggered while he/she is operating the machine, so it can be selectively deactivated by that specific machine's interrogator. The interrogator is designed to be powered by a  $12\text{V}$  vehicle power system. For many types of heavy equipment an external DC-DC converter would be required to convert a  $24\text{--}48\text{V}$  vehicle power source to the  $12\text{V}$  interrogator supply level. In most cases, if vehicle power failed, the heavy equipment would become disabled and therefore much less dangerous, so vehicle power failure could be permitted to interrupt the interrogator signal. However, some types of equipment might have significant stored kinetic or potential energy so an interrogator backup battery would be required in those cases.

### IV. RESULTS

In order to determine the maximum line-of-sight operating distance using the Friis transmission model, the RF sensitivity of the SmartHat was found using a dipole substitution test. This was done by first fixing the SmartHat at  $1\text{m}$  distance from the transmit antenna and then increasing the RF transmit power,  $P_t$ , until the turn-on threshold was reached and an audible tone was heard. Keeping the separation distance and transmit power constant, the SmartHat tag was replaced with a  $50\Omega$  dipole. The RF power developed by the dipole was measured with a spectrum analyzer. This substitution method is useful for non  $50\Omega$  systems such as the SmartHat tag and accounts for losses in the matching network and RF-to-DC conversion efficiency. The SmartHat's alert threshold including antenna gain was found to be  $\approx -8.48\text{dBm}$ . As summarized in Table I, the Friis propagation model predicts an operating distance of  $14.1\text{m}$ . In outdoor testing the SmartHat was observed to operate at distances of up to  $16.5\text{m}$ . This discrepancy is most likely due

TABLE I  
SMARTHAT TAG FORWARD LINK BUDGET

$\frac{P_r}{P_t} = G_t G_r \left( \frac{\lambda}{4\pi r} \right)^2$	
$P_t$	35 dBm
$G_t$	9 dBi
$G_r$	2.15 dBi
$\lambda$	33 cm
$r _{P_r = -8.48 \text{ dBm}}^\dagger$	14.1 m
$P_r _{r = 16.5 \text{ m}}^{\dagger\dagger}$	-9.8 dBm

<sup>†</sup> Observed by dipole substitution  
<sup>††</sup> Outdoor maximum distance

to differences in multipath between the indoor and outdoor environments.

## V. SUMMARY AND FUTURE WORK

An initial prototype SmartHat tag and interrogator device have been designed and constructed. The SmartHat tag includes a compact printed-circuit vee style antenna, an RF-to-DC power harvesting circuit, and a microprocessor-driven alert speaker. The tag's average operating power while delivering a pulsed alert is 1.8 V at 61  $\mu$ A, or 110  $\mu$ W (-9.6 dBm). Its power-up threshold when not delivering an alert is 1.8 V at  $\approx 10 \mu$ A. We also present a specialized interrogator device operating under FCC Part 18 rules in the 902-928 MHz band that is mounted to a piece of construction equipment to power and communicate with nearby SmartHats. Initial outdoor range testing indicates that the SmartHat tag will deliver an audio alert at distances of up to 16.46 m in unobstructed terrain when using an interrogator EIRP of +44 dBm, which is produced by an interrogator conducted output power of +35 dBm and a horizontally polarized Yagi antenna of 9 dBi gain.

More thorough testing will be conducted to understand system performance in different environments where increased multipath and terrain obstacles are present, and to validate that the SmartHat devices will survive the expected temperature, humidity, and vibration extremes expected in a real work site environment. The presence of severe multipath or terrain obstacles are the most likely impediments to the feasibility of a passively powered system, and will determine whether this type of system can achieve the high level of reliability required for a safety alert device. To mitigate adverse propagation effects, as well as improve alert reliability as a function of hard hat pose with respect to the heavy equipment, some type of local reservoir capacitance or a long life rechargeable battery could be considered for future SmartHat prototypes. For example, some types of lithium pentoxide rechargeable batteries have excellent performance over temperature and have a low self-discharge rate. Because alerts would be infrequent, the energy harvesting circuit would recharge the SmartHat's reservoir capacitor or battery in order to improve alert accuracy when sufficient link margin is present to receive the interrogator's messages even though insufficient forward-link power is present to operate the tag in alert mode. It will be necessary to evaluate the lifetime of any battery or reservoir capacitor chemistry under large numbers of charge/discharge

cycles and over extremes of temperature, humidity, and vibration to ensure that the reliability of the alert system could be maintained.

## VI. ACKNOWLEDGMENTS

This material is based in part upon work supported by the National Science Foundation under Grant Numbers CBET-0931924 and CMMI-0800858.

## REFERENCES

- [1] BodyGuard proximity warning system. Orbit Communications Pty Ltd. [Online]. Available: <http://www.orbitcoms.com/BodyGuard.php>
- [2] W. H. Schiffbauer and G. L. Mowrey, "An environmentally robust proximity warning system for hazardous areas," in *Proceedings of the ISA Emerging Technologies Conference 2001*. Instrument, Systems, and Automation Society, 2001, pp. 1–10.
- [3] ASE model 2200 proximity warning device. Allied Safety Engineering Inc. [Online]. Available: [http://www.alliedsafetyeng.com/proximity\\_warning\\_device.html](http://www.alliedsafetyeng.com/proximity_warning_device.html)
- [4] Energizer EN91 product datasheet. Energizer Holdings Inc. [Online]. Available: <http://data.energizer.com/PDFs/EN91.pdf>
- [5] Energizer L91 product datasheet. Energizer Holdings Inc. [Online]. Available: <http://data.energizer.com/PDFs/L91.pdf>
- [6] A. Sample, D. Yeager, P. Powledge, A. Mamishev, and J. Smith, "Design of an RFID-based battery-free programmable sensing platform," *IEEE Transactions on Instrumentation and Measurement*, vol. 57, no. 11, pp. 2608–2615, Nov. 2008.
- [7] D. Yeager, P. Powledge, R. Prasad, D. Wetherall, and J. Smith, "Wirelessly-charged UHF tags for sensor data collection," in *Proceedings of 2008 IEEE International Conference on RFID*, April 2008, pp. 320–327.
- [8] U. Karthaus and M. Fischer, "Fully integrated passive UHF RFID transponder IC with 16.7- $\mu$ W minimum RF input power," *IEEE Journal of Solid-State Circuits*, vol. 38, no. 10, pp. 1602–1608, October 2003.
- [9] G. De Vita and G. Iannaccone, "Design criteria for the RF section of UHF and microwave passive RFID transponders," *IEEE Transactions on Microwave Theory and Techniques*, vol. 53, no. 9, pp. 2978 – 2990, September 2005.
- [10] K. Seemann, F. Cilek, M. Schmidt, and R. Weigel, "RFID at UHF frequencies: The passive transponder frontend approach," in *International Conference on Microwaves, Radar & Wireless Communications, 2006. MIKON 2006.*, May 2006, pp. 657–661.